This is an electronic reprint of the original article.
This reprint may differ from the original in pagination and typographic detail.

Author(s): Tynell, Tommi & Yamauchi, Hisao & Karppinen, Maarit & Okazaki, Ryuji & Terasaki, Ichiro

Title: Atomic layer deposition of Al-doped ZnO thin films

Year: 2013

Version: Final published version

Please cite the original version:

Tynell, Tommi & Yamauchi, Hisao & Karppinen, Maarit & Okazaki, Ryuji & Terasaki, Ichiro. 2013. Atomic layer deposition of Al-doped ZnO thin films. Journal of Vacuum Science & Technology A: Vacuum, Surfaces, and Films. Volume 31, Issue 1. 01A109/1-4. ISSN 0734-2101 (printed). DOI: 10.1116/1.4757764.

Rights: © 2013 American Vacuum Society. This article may be downloaded for personal use only. Any other use requires prior permission of the authors and the American Institute of Physics. The following article appeared in Journal of Vacuum Science & Technology A: Vacuum, Surfaces, and Films. Volume 31, Issue 1 and may be found at http://scitation.aip.org/content/avs/journal/jvsta/31/1/10.1116/1.4757764.

All material supplied via Aaltodoc is protected by copyright and other intellectual property rights, and duplication or sale of all or part of any of the repository collections is not permitted, except that material may be duplicated by you for your research use or educational purposes in electronic or print form. You must obtain permission for any other use. Electronic or print copies may not be offered, whether for sale or otherwise to anyone who is not an authorised user.

Atomic layer deposition of Al-doped ZnO thin films

Tommi Tynell, Hisao Yamauchi, Maarit Karppinen, Ryuji Okazaki, and Ichiro Terasaki

Citation: Journal of Vacuum Science & Technology A **31**, 01A109 (2013); doi: 10.1116/1.4757764
View online: http://dx.doi.org/10.1116/1.4757764
View Table of Contents: http://scitation.aip.org/content/avs/journal/jvsta/31/1?ver=pdfcov
Published by the AVS: Science & Technology of Materials, Interfaces, and Processing

Articles you may be interested in

Low temperature atomic layer deposited Al-doped ZnO thin films and associated semiconducting properties
J. Vac. Sci. Technol. B **30**, 031210 (2012); 10.1116/1.4710519

Growth morphology and electrical/optical properties of Al-doped ZnO thin films grown by atomic layer deposition
J. Vac. Sci. Technol. A **30**, 021202 (2012); 10.1116/1.3687939

Effective atomic layer deposition procedure for Al-dopant distribution in ZnO thin films
J. Vac. Sci. Technol. A **28**, 1111 (2010); 10.1116/1.3460905

Structural, electrical, and optical properties of atomic layer deposition Al-doped ZnO films
J. Appl. Phys. **108**, 043504 (2010); 10.1063/1.3466987

Band-gap modified Al-doped Zn 1 − x Mg x O transparent conducting films deposited by pulsed laser deposition
Appl. Phys. Lett. **85**, 1374 (2004); 10.1063/1.1784544

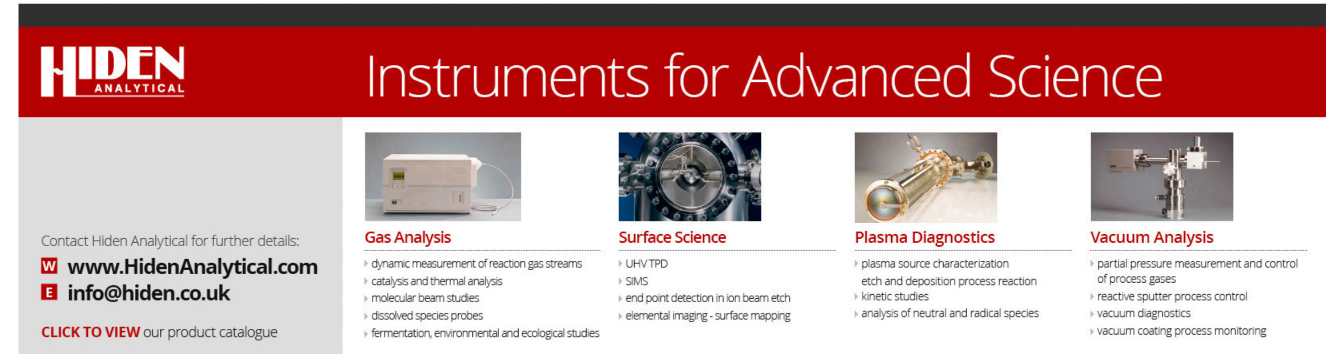

Redistribution subject to AVS license or copyright; see http://scitation.aip.org/termsconditions. Download to IP: 130.233.216.27 On: Wed, 14 Oct 2015 03:59:09

Atomic layer deposition of Al-doped ZnO thin films

Tommi Tynell, Hisao Yamauchi, and Maarit Karppinen[a)]
Department of Chemistry, Aalto University, FI-00076 Aalto, Finland

Ryuji Okazaki and Ichiro Terasaki
Department of Physics, Nagoya University, Nagoya 464-8602, Japan

(Received 1 August 2012; accepted 21 September 2012; published 10 October 2012)

Atomic layer deposition has been used to fabricate thin films of aluminum-doped ZnO by depositing interspersed layers of ZnO and Al_2O_3 on borosilicate glass substrates. The growth characteristics of the films have been investigated through x-ray diffraction, x-ray reflection, and x-ray fluorescence measurements, and the efficacy of the Al doping has been evaluated through optical reflectivity and Seebeck coefficient measurements. The Al doping is found to affect the carrier density of ZnO up to a nominal Al dopant content of 5 at. %. At nominal Al doping levels of 10 at. % and higher, the structure of the films is found to be strongly affected by the Al_2O_3 phase and no further carrier doping of ZnO is observed. © *2013 American Vacuum Society*. [http://dx.doi.org/10.1116/1.4757764]

I. INTRODUCTION

Zinc oxide is an n-type semiconductor that has great potential for use in many optoelectronic applications, particularly when doped with aluminum. The interest in Al-doped ZnO is due to its improved electrical conductivity without compromising the transparency of the material in the visible region of light,[1–4] which makes the material applicable as a transparent conductive oxide. Aluminum-doped ZnO has also been found to exhibit unusually good thermoelectric properties for an oxide, reaching a figure-of-merit value as high as 0.3 at 1000 K.[5,6] For both optoelectronic and thermoelectric applications, the accurate control of the charge carrier density is a priority; it directly affects not only the electrical conductivity but also the Seebeck coefficient and thermal conductivity, i.e., the three properties that define the figure-of-merit for a thermoelectric material.

Many of the applications proposed for Al-doped ZnO require the material to be prepared in thin film form, and the advantage of the atomic layer deposition (ALD) technique in producing uniform and conformal films with accurately controlled layer sequences makes it an ideal choice for realizing thin films with optimized carrier concentration values. The ALD technique has been successfully used in the past to deposit undoped and Al-doped ZnO thin films using diethyl zinc (DEZ), trimethyl aluminum (TMA), and water as the precursors.[7–14] In this work, we have investigated in detail the ALD process for depositing thin films of Al-doped ZnO and determined the extent of doping achievable using x-ray fluorescence, Seebeck coefficient, and optical reflectivity measurements.

II. EXPERIMENT

A. Thin film depositions

Thin films consisting of ZnO interspersed with regularly spaced single layers of Al_2O_3 were deposited in an appropriate pulse ratio to achieve ZnO films with a nominal Al dopant content of 0–20 at. %. A Picosun R-100 reactor was used for the depositions, and the precursors were DEZ and H_2O for the ZnO growth cycles and TMA and H_2O for the Al_2O_3 growth cycles. Borosilicate glass, which had been cleaned beforehand by ultrasonic cleaning in H_2O (twice) and ethanol (once), as well as Si were used as the substrates in all depositions. The precursors were unheated, and the substrate temperature was 220 °C for all the depositions. All depositions consisted of 600 cycles of DEZ/H_2O and TMA/H_2O in total with pulsing times of 0.1 s for DEZ and H_2O and 0.3 s for TMA. All precursor pulses were followed with N_2 purges of 4.0 s for DEZ and H_2O and 6.0 s for TMA.

B. Sample characterization

The crystal structure and thickness of the films deposited on borosilicate substrates were determined with the PANalytical X'Pert Pro x-ray diffractometer (Cu K_α radiation) using the grazing incidence x-ray diffraction (GIXRD) and x-ray reflection (XRR) techniques, respectively. A Philips PW 1480 x-ray spectrometer was used to perform x-ray fluorescence (XRF) measurements on the films deposited on Si substrates to determine their metal composition.

Optical reflectivity measurements were carried out at room temperature for the films deposited on borosilicate substrates using a Jasco IRT-5000 Irtron Infrared Microscope in the energy range of 0.06–1.3 eV. Two measurements were performed for each sample to acquire the reflectivity data: one for the near-IR range (0.27–1.3 eV) and one for the mid-IR range (0.06–0.97 eV). A halogen lamp was used as the light source for the near-IR range measurements, while a ceramic light source was used for the mid-IR range measurements. To determine the absolute value of the reflectivity, a silver mirror was used for measuring the reference spectrum.

Seebeck coefficient measurements were performed in a temperature range of 5–300 K for the films deposited on borosilicate using a homemade system. The measurements were done by fixing the sample between two copper plates using silver paste and applying a temperature gradient of 0.5–1.5 K over the sample by heating one of the plates. Cooling of the measurement system was achieved by slowly lowering the system into a tank of liquid helium.

[a)]Electronic mail: maarit.karppinen@aalto.fi

 0734-2101/2013/31(1)/01A109/4/$30.00 © 2013 American Vacuum Society

Redistribution subject to AVS license or copyright; see http://scitation.aip.org/termsconditions. Download to IP: 130.233.216.27 On: Wed, 14 Oct 2015 03:59:09

III. RESULTS AND DISCUSSION

A. Growth characteristics

All the depositions produced uniform films. The appearance of the as-deposited ZnO films was blue for the samples deposited on Si and bluish for the ones deposited on borosilicate substrates. As the number of TMA/H_2O pulses in the deposition program was increased, the color of the resulting films stayed approximately the same for low dopant concentrations but shifted toward a darker blue for the 10 at. % Al-doped films and brown for the 20 at. % Al-doped films.

X-ray diffraction patterns of the as-deposited films are shown in Fig. 1. All the diffraction peaks could be indexed according to the wurtzite structure of ZnO. From Fig. 1, it can be observed that at low dopant concentrations the Al doping has little effect on the XRD pattern of the parent ZnO phase. At higher levels of Al doping, the film is more amorphous in character as can be seen for the 10 at. % film in Fig. 1, which shows only the (100) and (110) peaks of the ZnO wurtzite structure clearly, with only traces of the other peaks remaining. The film with nominal 20 at. % Al doping is already completely amorphous, and no sign of the ZnO wurtzite structure can be seen in the XRD pattern.

The growth per cycle (GPC) values for the depositions with different pulsing ratios are shown in Fig. 2. The GPC values for the lower Al-content films fluctuate around 1.5 Å/cycle until the film with nominal Al doping of 10 at. %, but the film with 20 at. % Al shows a growth rate that is clearly lower than the rest. The difference is so large that it cannot be explained merely by a slower growth rate of Al_2O_3 compared to that of ZnO, especially since the nominally 10 at. % Al-doped film has a similar growth rate to the pure ZnO and the films with low Al contents. Therefore, the frequent TMA/H_2O pulses in the growth sequence must be hindering the growth of the parent ZnO phase, thus resulting in a considerably thinner film compared to the other depositions. The observed GPC values of 1.5–1.6 Å for ZnO and the films with low Al dopant concentrations are in good agreement with values from previous studies.[8,15,16]

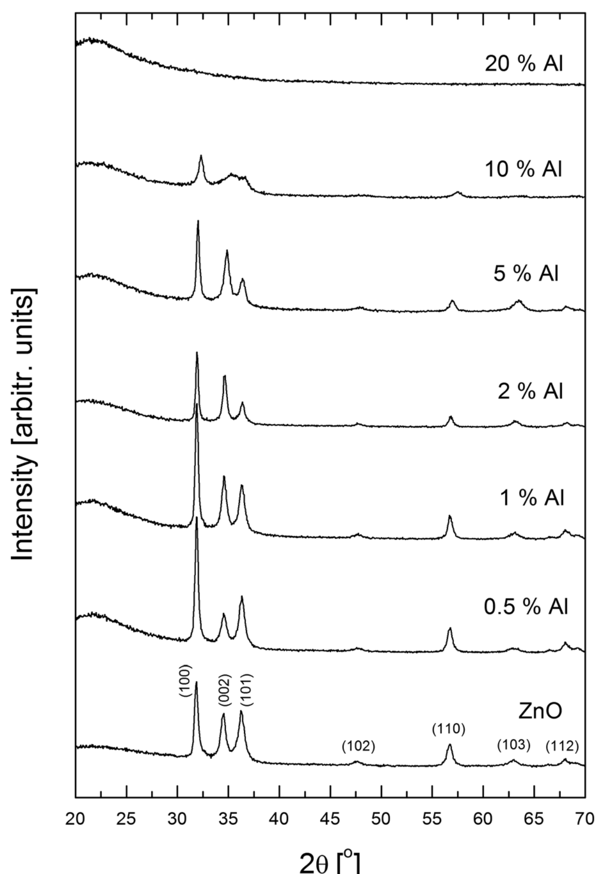

FIG. 1. XRD patterns for the ZnO films with different nominal Al contents. The indices are for the wurtzite structure of ZnO.

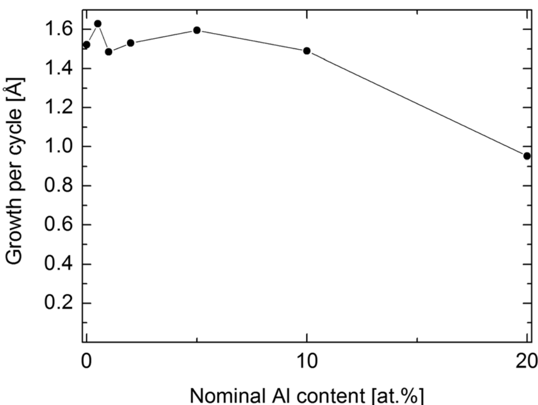

FIG. 2. GPC for the ZnO films with different nominal Al contents.

The XRF measurements revealed a nonlinear relation between the nominal dopant concentration and the actual atom percentage of Al observed in the films (Fig. 3). The increase in the Al content of the films is fairly consistent with the nominal dopant concentration at low levels of doping, but the 10 at. % Al-doped film already shows an actual Al content of more than double the intended amount, and at the 20 at. % level, the observed Al content is over 70 at. %. The extremely large difference between the intended and actual Al content also supports the hypothesis that the ZnO growth is being hindered by the frequent Al_2O_3 layers. The

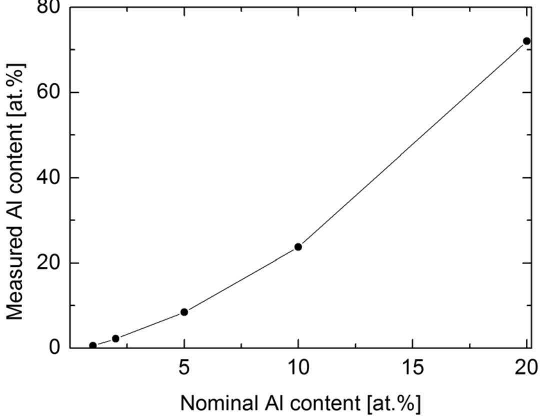

FIG. 3. Actual Al content of the variously doped ZnO films (measured with XRF) compared to the nominal Al content.

Redistribution subject to AVS license or copyright; see http://scitation.aip.org/termsconditions. Download to IP: 130.233.216.27 On: Wed, 14 Oct 2015 03:59:09

observed high Al content is in line with previous results by Banerjee *et al.*,[9] where the actual Al content was also found to be unexpectedly high at larger dopant concentrations. Elam *et al.*[17] have suggested a mechanism by which the TMA precursor can etch Zn from the film, which would explain the reduction in the Zn content of the film.

Taken together, the XRD, XRR, and XRF measurements reveal that the ALD process works well in doping ZnO with Al until the 5 at. % level, the measurements showing no changes in the crystal structure, a fairly constant growth rate, and a linear Al content response to doping. At the nominal Al content of 10 at. %, the XRD pattern shows little sign of the wurtzite structure and the relatively high Al content of over 20 at. % from XRF indicates that the ZnO growth is already being hindered and the amorphous structure of Al_2O_3 is starting to become dominant. The film with the nominal 20 at. % Al doping is completely amorphous and has a very high Al content. Also for this film the growth rate was greatly reduced. All these factors indicate that the Al_2O_3 phase has become dominant and hindered the growth of ZnO so much that the resulting film is more Al_2O_3 than ZnO.

B. Physical properties

The Seebeck coefficient data measured for the films in the temperature range of 5–300 K are displayed in Fig. 4. There is a clear shift in the Seebeck coefficient values of the films that is dependent on the dopant concentration and is consistent with a rise in the carrier density. As the dopant concentration increases, the absolute value of the Seebeck coefficient decreases, reaching a minimum in the nominally 5 at. % Al-doped film. The 10 at. % Al-doped film displays no further decrease, indicating that a limit has been reached in the solubility of Al into ZnO and thus no decrease in the Seebeck coefficient is observed. The measurement could not be performed at all for the film with nominal Al content of 20 at. %, presumably because of the high electrical resistivity of the film, which interferes with the measurement. The observed absolute values of Seebeck coefficient are somewhat low compared to reported values for bulk samples[18] but correspond well to those reported for thin films.[19]

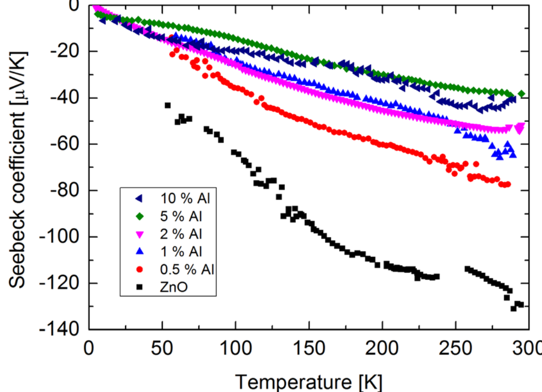

Fig. 4. (Color online) Seebeck coefficient data for the ZnO films with different nominal Al contents.

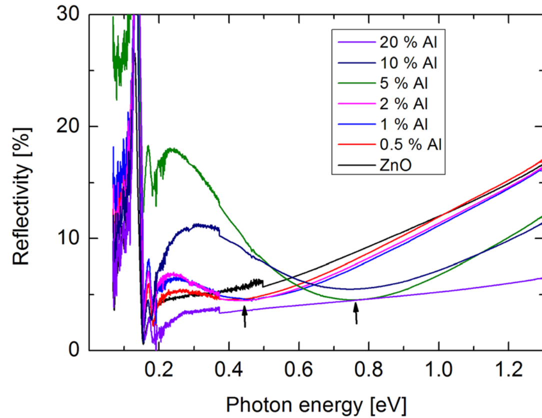

Fig. 5. (Color online) Reflectivity spectra for the ZnO films with different nominal Al contents, where the arrows point out the positions of the Drude edge for the 2 at. % and 5 at. %-doped films.

The reflectivity spectra for the Al-doped ZnO films are shown in Fig. 5. Upon the Al doping a so-called Drude edge (indicated in Fig. 5 with arrows) appears. It is moreover seen that the position of the edge shifts to higher energies with increasing Al dopant concentration. The Drude edge, i.e., a minimum in the reflectivity spectrum, determines the plasma frequency, ω_p, of the electron gas in the film, and thus, it can be used to estimate the charge carrier density of the films according to the following equation:

$$\omega_p = \left(\frac{ne^2}{m^* \varepsilon_\infty}\right)^{\frac{1}{2}}, \tag{1}$$

where n is the carrier density, e is the electron charge, m^* is the effective mass of the charge carriers, and ε_∞ is the high-frequency permittivity. The shift of the Drude edge to higher energies with higher Al content observed in Fig. 5 thus corresponds to a rise in the carrier density of the films. This carrier density increase can be observed up to a nominal Al content of 5 at. %, after which the position of the Drude edge remains the same for the film with 10 at. % Al, indicating that no further carrier doping has been achieved. No Drude edge can be seen at all for the nominally 20 at. % Al-doped film, which would be expected for a film consisting mostly of Al_2O_3.

The Seebeck coefficient and optical reflectivity measurements both indicate that the charge carrier density of the ZnO films can be increased with the inclusion of TMA/H_2O pulses in between the DEZ/H_2O pulses of the deposition process. The limit for this carrier doping is around a nominal Al content of 5 at. %, as can be seen in both the Seebeck coefficient and reflectivity data.

IV. SUMMARY AND CONCLUSIONS

In this work, we have demonstrated the viability of using ALD to dope ZnO films with relatively large amounts of aluminum. X-ray diffraction patterns of the films confirmed that the wurtzite crystal structure of ZnO remained intact up to a nominal Al content of 5 at. %. X-ray fluorescence measurements revealed that the actual Al content of the films greatly

Redistribution subject to AVS license or copyright; see http://scitation.aip.org/termsconditions. Download to IP: 130.233.216.27 On: Wed, 14 Oct 2015 03:59:09

increases once the nominal Al content is increased above 5 at. %, and x-ray reflectivity measurements showed a corresponding decrease in the film growth rate. This indicates that the ZnO growth is hindered if the ratio of TMA/H_2O pulses in the deposition process is increased above 1:20.

Optical reflectivity and Seebeck coefficient measurements showed an increase in the charge carrier density of the films as the dopant content was increased, which confirms that the inclusion of Al into the films resulted in carrier doping of the ZnO structure. This effect was observed up to a nominal dopant content of 5 at. %, suggesting that the limit for homogeneous doping of Al into ZnO lies somewhere around 5 at. %

ACKNOWLEDGMENTS

This work was supported by grants from TEKES (Grant Nos. 1726/31/07 and 3211/31/2009), Academy of Finland (Grant Nos. 130352 and 255562) and the Scandinavia-Japan Sasakawa Foundation.

[1]T. Minami, H. Sato, T. Sonoda, H. Nanto, and S. Takata, Thin Solid Films **171**, 307 (1989).
[2]A. Kuroyanagi, Jpn. J. Appl. Phys., Part 1 **28**, 219 (1989).
[3]J. Mass, P. Bhattacharya, and R. S. Katiyar, Mater. Sci. Eng. B **103**, 9 (2003).
[4]S. H. Jeong, B. N. Park, D.-G. Yoo, D. Jung, and J.-H. Boo, J. Korean Phys. Soc. **50**, 622 (2007).
[5]M. Ohtaki, T. Tsubota, K. Eguchi, and H. Arai, J. Appl. Phys. **79**, 1816 (1996).
[6]T. Tsubota, M. Ohtaki, K. Eguchi, and H. Arai, J. Mater. Chem. **7**, 85 (1997).
[7]V. Lujala, J. Skarp, M. Tammenmaa, and T. Suntola, Appl. Surf. Sci. **82/83**, 34 (1994).
[8]J. W. Elam and S. M. George, Chem. Mater. **15**, 1020 (2003).
[9]P. Banerjee, W.-J. Lee, K.-R. Bae, S. B. Lee, and G. W. Rubloff, J. Appl. Phys. **108**, 043504 (2010).
[10]N. P. Dasgupta, S. Neubert, W. Lee, O. Trejo, J.-R. Lee, and F. B. Prinz, Chem. Mater. **22**, 4769 (2010).
[11]B. Sang and M. Konakai, Jpn. J. Appl. Phys., Part 2 **35**, L602 (1996).
[12]E. B. Yousfi, J. Fouache, and D. Lincot, Appl. Surf. Sci. **153**, 223 (2000).
[13]E. Guziewicz *et al.*, J. Appl. Phys. **103**, 033515 (2008).
[14]G. Luka, L. Wachnicki, B. S. Witkowski, T. A. Krajewski, R. Jakiela, E. Guziewicz, and M. Godlewski, Mater. Sci. Eng. B **176**, 237 (2011).
[15]A. W. Ott and R. P. H. Chang, Mater. Chem. Phys. **58**, 132 (1999).
[16]B.-Y. Oh *et al.*, Curr. Appl. Phys. **12**, 273 (2012).
[17]J. W. Elam, D. Routkevitch, and S. M. George, J. Electrochem. Soc. **150**, G339 (2003).
[18]K. F. Cai, E. Müller, C. Drašar, and A. Mrotzek, Mater. Sci. Eng. B **104**, 45 (2003).
[19]N. Ma, J.-F. Li, B. P. Zhang, Y. H. Lin, L. R. Ren, and G. F. Chen, J. Phys. Chem. Solids **71**, 1344 (2010).

Redistribution subject to AVS license or copyright; see http://scitation.aip.org/termsconditions. Download to IP: 130.233.216.27 On: Wed, 14 Oct 2015 03:59:09